JOURNAL OF MATERIALS SCIENCE 37 (2002) 2623–2633

Effect of thermal ageing on Nylon 6,6 fibres

A. JAIN, K. VIJAYAN*
Materials Science Division, National Aerospace Laboratories, Bangalore 560 017, India
E-mail: Kavi@css.cmmacs.ernet.in

The residual effects of thermal ageing at various temperatures on fibres of the aliphatic polyamide Nylon 6,6 have been studied. Both crystal and macro structural characteristics manifest the residual effects. The former category includes changes in intensity, *2θ* values and half width. The macro changes include introduction of surface damages in the form of holes, material deposits etc. The fibre also undergoes reduction in weight. The structural changes suggest deterioration in the initial tensile characteristics which has been verified experimentally. A direct correlation between the tensile strength and the angular separation of the equatorial reflections has also been observed. © *2002 Kluwer Academic Publishers*

1. Introduction

Nylon 6,6 is an aliphatic amide made up of poly (hexamethylene adipamide). The structural formula of Nylon 6,6 is shown below.

$$[-(CH_2)_6 - NH-CO - (CH_2)_4 - CO-NH-]_n$$

Nylons have an extensive range of applications viz., as apparel, carpets, tyre reinforcement, parachutes and many other industrial applications. Nylon 6,6 is recommended for use upto 100°C [1]. Do exposures to elevated temperatures affect the initial characteristics of the fibre? This paper reports the residual effects of cumulative thermal exposures or thermal ageing on the initial characteristics of commercially available Nylon 6,6 fibres derived by X-ray diffraction methods, scanning electron microscopy, tensile testing and weight analysis. It must be mentioned that to date, data on the residual effects of thermal ageing on Nylon 6,6 fibres are not available. Radusch *et al.*'s [2] X-ray analysis on Nylon 6,6 at elevated temperatures has been carried out with an *in situ* heating arrangement and it therefore differs from the present study which concerns the residual effects. It must also be mentioned that in the past, extensive investigations have been carried out on the thermal ageing behavior of the aromatic polyamides Kevlar, Nomex and Twaron [3–12]. In this context, it was also of interest to find out whether the behaviors of the aliphatic and the aromatic polyamides were comparable.

2. Experimental details

The Nylon 6,6 fibres used in this study were obtained from M/s Goodfellow. Thermal ageing was conducted at three different temperatures *(T)* viz., 175, 225 and 245°C respectively. It must be pointed out that the choice of T's above 100°C was deliberate and was intended to enable accelerated data collection. The total duration of cumulative exposure, $t_{cum}(T)$ varied with T. Table I lists the T and $t_{cum}(T)$ values chosen. Unconstrained bundles of Nylon 6,6 fibres were aged in air using a tubular resistance furnace which can maintain the temperature to an accuracy of ±2°C. Prior to and at various stages of ageing, the fibres were characterized using various techniques viz., X-ray diffraction, weight analysis, scanning electron microscopy and tensile testing.

Wide angle X-ray diffraction patterns were recorded in the reflection geometry, using a Philips powder diffractometer with a proportional counter and a graphite monochromator in the diffracted beam. Cu K_α radiation was used. The samples were rotated at a rate of 1/4° per minute and a chart speed of 10 mm per minute was used. In the equatorial X-ray diffraction pattern from Nylon 6,6, the two most intense reflections are (100) and ((010) + (110)) occurring at *2θ* values of ~20.4° and 23.4 respectively, for Cu K_α radiation. The overlapping reflections $(\bar{1}\,10)$ and (210) occurring at *2θ* value of ~41.3° are comparatively very weak. The recording of the equatorial X-ray diffraction patterns was therefore confined to the *2θ* range of 14 to 30°. The indices of the reflections mentioned above are based on the triclinic unit cell of dimensions a = 4.9, b = 5.4 and c = 17.2 Å, a = 48.5, ft = 77 and y = 63.5° reported by Bunn and Garner [13]. The parameters $2\theta_{max}$ values, half width (ω) and integrated intensity (I) characterizing the diffraction profiles were obtained by fitting a Lorentzian^2 function. As is well known, the integrated intensities are related to the crystallinity of the diffracting sample [14]. As the present study concerns only relative changes in crystallinity, no attempt was made to estimate the absolute values of crystallinity. However, the parameter $k = I_t(T)/I_0$, was used to identify the residual crystallinity of thermally aged fibres. In the above expression for k, the parameters I_0 and $I_t(T)$ correspond to the total integrated intensities of the reflections recorded from fibres prior to and at various stages of heat treatment respectively.

*Author to whom all correspondence should be addressed.

TABLE I T and $t_{cum}(T)$ values chosen for analysis

Temperature (T) (°C)	$t_{cum}(T)$ <h>
175	200, 350, 450, 800, 1000, 1350, 1500, 1750
225	1, 2, 5, 30, 15, 18, 20, 22
245	1, 3, 5, 7, 10, 12, 14, 16

The percentage variation in weight accompanying thermal ageing was estimated as $(\Delta w/w_0)$ x 100, using a Sartorius analytical balance capable of reading down to 0.0001 g. Here, $\Delta w = WQ - w_t$, w_0 and w_t are the weights of samples prior to and after heat treatment respectively. The latter weight was measured within five minutes of removing the sample from the furnace and cooling to ambient temperature. For each of the chosen experimental conditions, at least three sets of samples were examined and the average value of weight loss was worked out. A Leo scanning electron microscope was used to examine the structural features of gold coated fibres. It must be emphasized that care was taken to avoid manually introduced artifacts and deformations. Prior to examination in the microscope, the surface of fibres was not touched or subjected to any type of bending, twisting etc. Tensile strength, modulus and percentage elongation at break of individual filaments were estimated using a Zwick universal testing machine. For each of the experimental conditions, at least 50 filaments were examined and the average values of tensile properties were estimated.

3. Results and discussion

3.1. X-ray diffraction

Fig. 1a–c present the diffraction patterns recorded prior to and at various stages of ageing at 175, 225 and 245°C respectively. It must be pointed out that Nylon 6,6 has *a* as well as *ft* forms [13]. The *a* form is, however, the commonly occurring phase. Partial inclusion of the *ft* form in the sample used in the present study has been ruled out by checking for the reflections from the *ft* form. In particular, the nonoccurrence of the reflections at *26* values of ~12 and 19° confirmed the absence of the *ft* form in the sample. The dimensions of the triclinic unit cell characterizing the β form are $a = 4.9$, $b = 8.0$ and $c = 17.2$Å, $\alpha = 90$, $ft = 77$ and $\gamma = 67°$ [131.

3.1.1. Intensities

The diffraction patterns in Fig. 1a–c show that the intensities manifest a progressive variation with temperature as well as the duration of cumulative exposures. It is found that at each of the chosen temperatures, at some stage of the prolonged thermal exposures, the intensities of reflections reach values where they are no longer observable above the background i.e., at this stage of thermal exposure, the sample has no crystalline fraction left to diffract. This stage is referred to as the zero crystallinity state. The time needed for the 100% loss in crystallinity is referred to as t_{100}. It must be emphasized that the zero crystallinity state is reached as a result of cumulative exposure to a constant temperature. It is found that at 175, 225 and 275°C ≈ 1750, 22 and 16 h respectively of exposures are needed to reach the zero crystallinity state. Fig. 2 presents the logarithmic variation of t_{100} with T.

Values of k depicting the progressive diminution and an eventual total loss in crystallinity have been marked in each set of the diffraction patterns in Fig. 1. From these values, the time needed for 50% reduction in the initial crystallinity, t_{50}, has been derived and included in Fig. 2. The parameters t_{50} and t_{100} are indeed user relevant because from an extra/interpolation of the curves in Fig. 2, it is possible to predict the duration of exposure which will cause any deterioration in the initial crystallinity, for a chosen T value. As is well known, crystallinity is an important characteristic related to the properties of fibres. Variation in crystallinity introduced by isothermal ageing of the type conducted in the present study implies corresponding changes in properties which in turn can affect the performance of the fibre during its service life.

Fig. 1 shows that prior to reaching the zero crystallinity state, the relative intensities of the two most intense reflections exhibit an interesting behavior. As can be seen in the patterns from the as received fibres i.e., prior to heat treatment, the peak intensity, $I_{p(010)+(110)} \approx I_{p(100)}$. However, with continuance of thermal exposures, the relative I_p values change. At both 225 and 245°C, the difference between the I_p values reaches a high after 5-7 h of thermal exposure. At this stage, $I_{p(010)+(110)} > I_{p(100)}$. Beyond this stage there is an overall reduction in the integrated intensities leading, eventually, to a state of nearly zero intensity. As is well known the intensity distribution in an X-ray diffraction pattern depends on the atomic and molecular arrangement. The observations on the time dependent variations in relative intensities suggest that the first few thermal exposures of Nylon 6,6 cause changes in the atomic/molecular arrangement which in turn lead to changes in the relative intensities of the equatorial reflections. Subsequent exposures, however, cause progressive degradation and an eventual total loss in the crystallinity of the fibre.

3.1.2. 2θ values

It must be pointed out that in the patterns shown in Fig. 1, the ((010) + (110)) reflections occur at 2θ less than the value reported by Bunn and Garner [13] viz., shifted towards the low angle side by ~0.5° on the *29* scale. This feature suggests that the *b*-dimension characterizing the samples used in the present study is slightly more than what has been reported for Nylon 6,6 [13]. In the crystal structure of Nylon 6,6 the hydrogen-bonded layers are stacked along the crystallographic *b*-direction. The enhanced *b*-value thus suggests that the layers are, initially, farther apart than expected.

Fig. 3 presents the variation of *28* values with T and $t_{cum}(T)$ values. It is observed that *29* values for both the reflections increase initially followed by a decrease. The initial increase which suggests a reduction in the corresponding interplanar spacing (d) could be interpreted as an initial annealing type of effect introduced

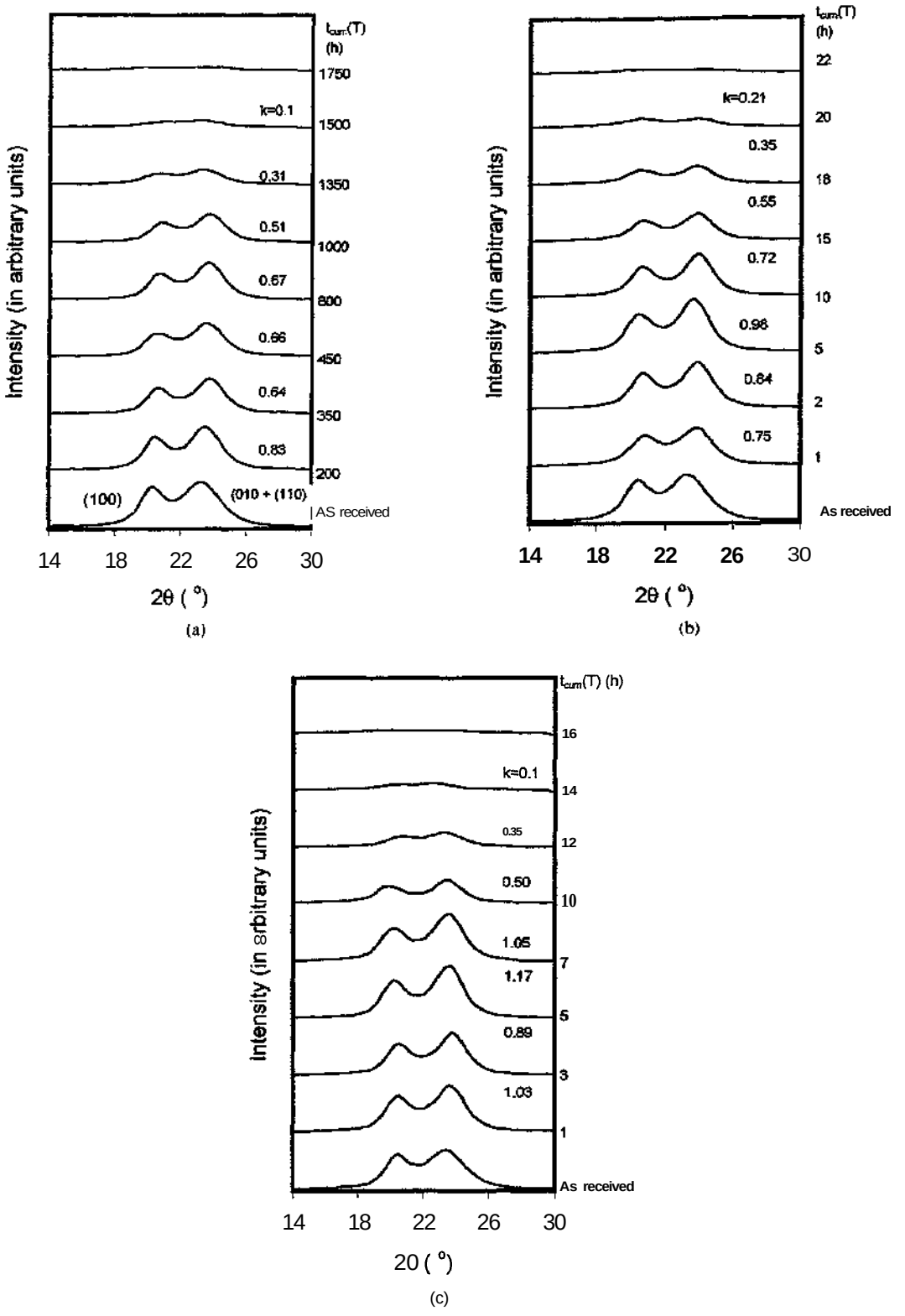

Figure 1 (a) X-ray diffraction profiles recorded prior to and at various stages of exposure to 175°C. (b) X-ray diffraction profiles recorded prior to and at various stages of exposure to 225°C. (c) X-ray diffraction profiles recorded prior to and at various stages of exposure to 245°C.

by thermal exposures. The subsequent increase in the d-spacing may be associated with the residual effects of thermal expansion which have occurred at the respective elevated temperatures.

The observed shifts in the *2θ* values of the equatorial reflections recorded from thermally aged Nylon 6,6 fibres are strikingly different from Radusch *et al.*'s [2] observations. Radusch *et al.*'s X-ray analysis using an *in situ* heating arrangement has shown that the two reflections (100) and (010) + (110) shift in opposite directions i.e. whereas the $d_{(100)}$ spacing decreased with temperature, the $d_{(010)+(110)}$ spacing increased. Radusch *et al.* mention that with progressive shifts occurring in opposite directions, the two equatorial reflections coalesce at ~207°C. The merging of reflections is attributed to a triclinic → psuedo hexagonal structural transformation. The observed reduction in the d-spacing is also interpreted as partial breaking

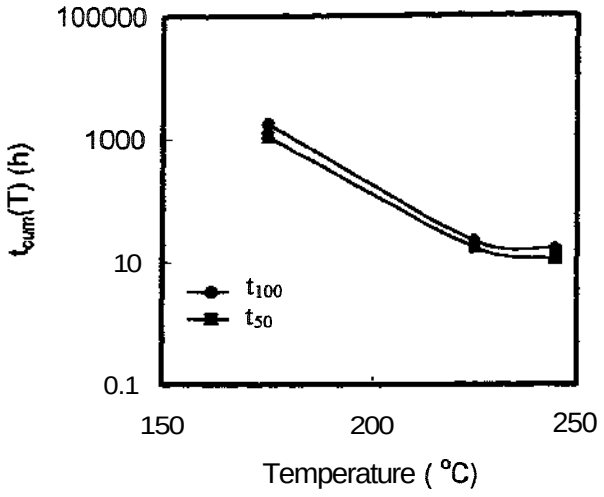

Figure 2 t_{100} and t_{50} vs. T. Here, t_{100} and t_{50} refer to the respective cumulative exposure time needed for 100 and 50% reduction in crystallinity.

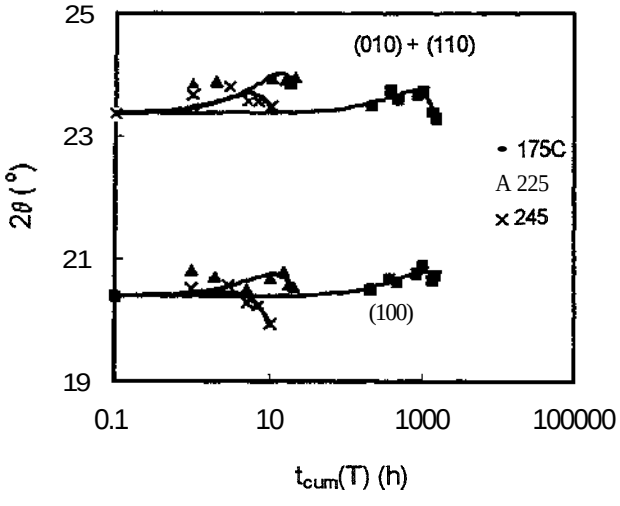

Figure 3 Variation of *28* values with $t_{cum}(T)$ and T.

of hydrogen bonds and changes in their orientation. It must be emphasized here that these observations pertain to data collected at the respective elevated temperatures with an *in situ* heating arrangement.

In contrast with the *in situ* heating studies of Radusch *et al.* [2], the present investigation concerns the residual effects of heating. As can be seen from Fig. 1, the two equatorial reflections remain distinct at all stages of thermal ageing. The present set of data establishes that the residual effect does not include any merging of reflections at any stage of thermal ageing. It may therefore be surmised that even if the fibres have undergone the triclinic → psuedo hexagonal structural transformations at elevated temperatures, the transformation is reversible. On returning to ambient temperatures, where the X-ray diffraction patterns were recorded, the samples are back to the triclinic phase albeit with slight shifts in the unit cell dimensions (Fig. 3).

A parameter which is determined by the *20* values of the two equatorial reflections is the angular separation A(20) defined as A(20) $= 2\theta_{(010)+(110)} - 2\theta_{(100)}$. In the case of Kevlar 49 fibres it has been reported that the

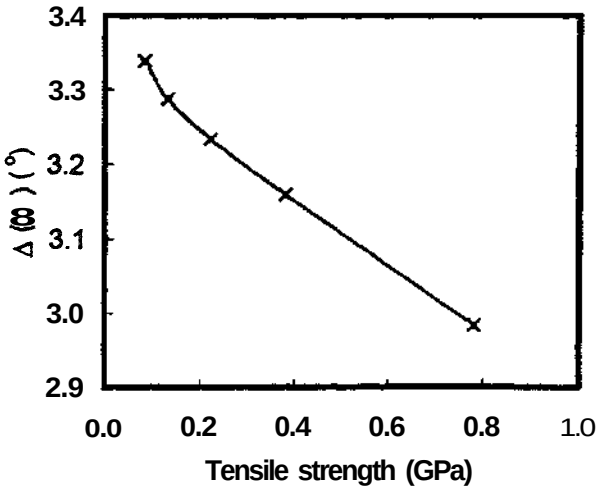

Figure 4 $\Delta(2\theta)$ vs. tensile strength for Nylon 6,6 fibres aged at 245°C.

angular separation of the equatorial reflections (200) and (110) is closely related to the tensile strength of the fibre [15] viz., the two equatorial reflections were found to get closer with reduction in tensile strength. A direct correlation between the A(20) values and the tensile strength is indeed a very useful parameter for quickly assessing or monitoring the tensile strength of large batches of fibres. With this point in view, the A(20) values and the tensile strength of Nylon 6,6 fibres were also examined and a correlation has indeed been observed. Fig. 4 records the direct correlation between the A(20) and the tensile strength of fibres aged at 245°C. Details of the estimation of tensile strength will be presented in a later section of this paper. The striking difference between Nylon 6,6 and Kevlar fibres is that in the former, reduction in tensile strength is accompanied by an increment in angular separation (Fig. 4). In contrast, in Kevlar, the angular separation decreases with reduction in tensile strength. This difference in the nature of correlations could be speculated to be due to probable differences in the load bearing mechanisms in the crystal structures of both the fibres.

3.1.3. Half width, ω

Fig. 5 presents the observed variations, ω/ω_0, in the half widths of the reflections. Here, ω_0 and *CD* refer to the half widths of reflections prior to and after thermal exposures respectively. The halfwidth of reflection (100) remains nearly unaffected in the early stages of exposures. However, the subsequent broadening suggests fragmentation of crystallites and/or increase in microstrain [14]. In the case of the second profile, the behavior is slightly different. There is evidence for a slight, initial sharpening indicating improvement in crystallite size and/or reduction in microstrain. With further continuance of thermal exposures, the reflections (010) + (110) tend to broaden thereby suggesting fragmentation of crystallites and/or build up of microstrain. It is also found that the changes in the half width values are not identical for the two equatorial reflections. The broadening introduced in the (100) profile is much more than

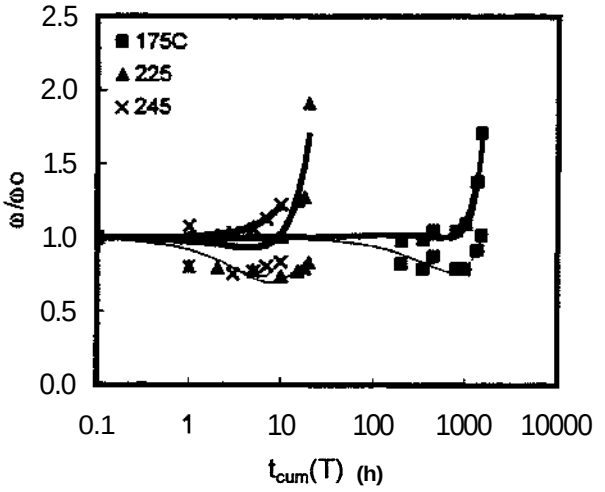

Figure 5 Fractional variation in the half width values. — (100) and — (010) + (110).

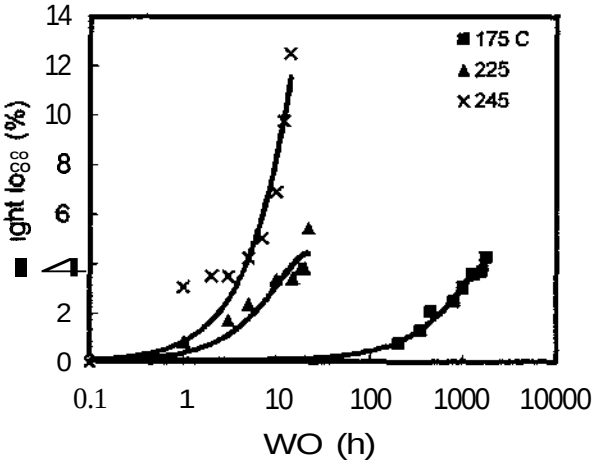

Figure 6 Weight loss (%) for various T and $t_{cum}(T)$ values.

in the combined profiles ((010) + (110)). The preferentially large changes in the half width of the reflection (100) suggest that the (100) set of planes are perhaps structurally more sensitive to thermally induced changes. Similar preferential changes were observed in thermally aged Kevlar fibres also where, of the two equatorial reflections (200) and (110), the latter manifested enhanced sharpening [3, 5].

It may also be pointed out that on the time scale, the stage at which the sharpening terminates and broadening starts, varies with T. At higher temperatures, the change over from sharpening to broadening takes place comparatively early.

3.2. Weight analysis

Fig. 6 presents the results on the weight loss. It is found that increase in temperature causes enhanced weight loss. In addition, for a constant value of T, increase in the $t_{cum}(T)$ value also causes a progressive reduction in weight i.e. during any high temperature application, if the fibres are used at a fixed temperature for long durations, it will undergo a progressive weight loss. The above-mentioned data on weight loss values pertain to thermal exposures carried out in air. Exposures in controlled atmospheres like nitrogen gas may be expected to alleviate the deterioration.

The weight loss suggests that thermal exposures have led to material loss which can be a consequence of thermally induced chemical degradation. As the present study does not include chemical analysis, further information on possible chemical degradation induced by thermal exposures is not available. However, the features of the micrographs to be described in the next section provide evidence for evolution of materials, perhaps a consequence of chemical degradation, in thermally aged samples. Weight loss of the type described above can indeed be expected to lead to changes in the initial tensile characteristics of the fibre, the details of which are presented later in this paper.

3.3. Scanning electron micrographs (SEMicrographs)

The characteristics of Nylon 6,6 fibres deciphered from scanning electron micrographs are summarized below. Attention was focused, primarily, to identify the surface characteristics. Some information on the nature of the tensile fracture has also been obtained.

3.3.1. Prior to thermal exposures or the 'as received' fibres

Prior to heat treatment, faint lines parallel to the fibre length have been observed on the surface (Fig. 7a). It is likely that these lines are related to the conditions of processing of fibres. Very tiny specks of some extraneous material are also found to be randomly distributed on the surface. These two features suggest that the surface of the 'as received' fibres cannot be described as 'featureless'. The micrograph in Fig. 7b represents the typical tensile fracture behavior of an as received Nylon 6,6 fibre.

3.3.2. Fibres aged at 175°C

Formation of large number of holes and groovelike openings on the surface of fibres aged at 175°C for 1750 h has been shown in Figs 8 and 9 respectively. The latter feature has been shown by arrows A and B in Fig. 9. In comparison with the as received fibre, the deposit of extraneous material has also increased slightly in fibres exposed to 175°C. Fig. 8 depicts the brittle nature of the tensile fracture. The initially flexible Nylon 6,6 fibre has turned brittle after prolonged exposure to 175°C.

3.3.3. Fibres aged at 225°C

The enhancement of surface deposits in fibres aged at 225°C can be appreciated from Figs 10 and 11. The former shows an extensive deposit engulfing the surface. The surface also depicts increase in the number as well the size of the holes. In contrast with the randomly distributed holes shown in Fig. 10, the micrograph in Fig. 12 shows a localized deep pit. Another interesting feature observed in the micrograph in Fig. 13 concerns a longitudinal degradation/failure. Along the line seen in the micrograph, extensive damage appears to have

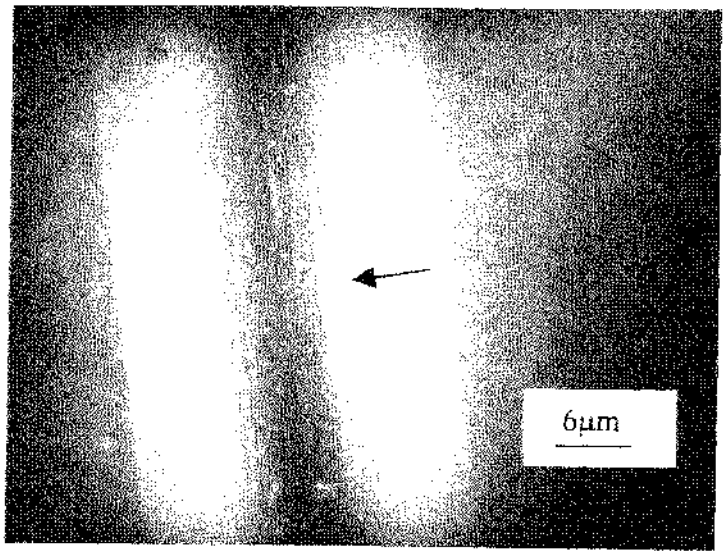

(a)

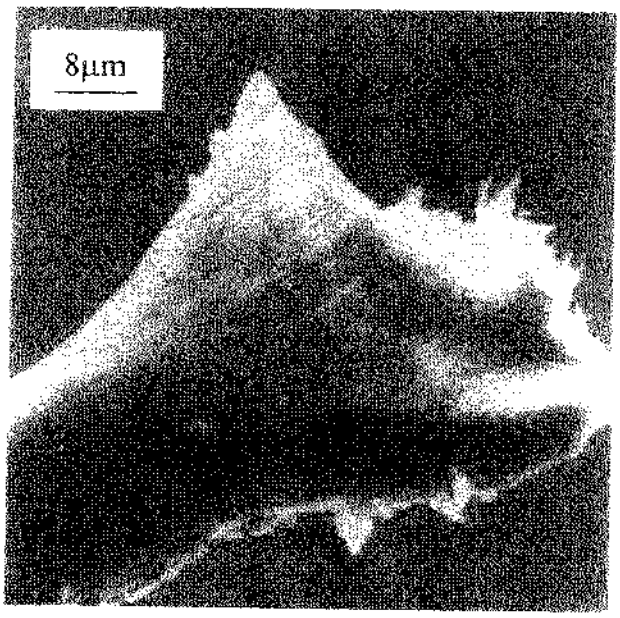

(b)

Figure 7 (a) SEMicrograph showing the surface of a Nylon 6,6 fibre, prior to thermal exposure. Arrow shows a line on the surface. (b) SEMicrograph representing the typical tensile fracture behaviour of a fibre prior to thermal exposure.

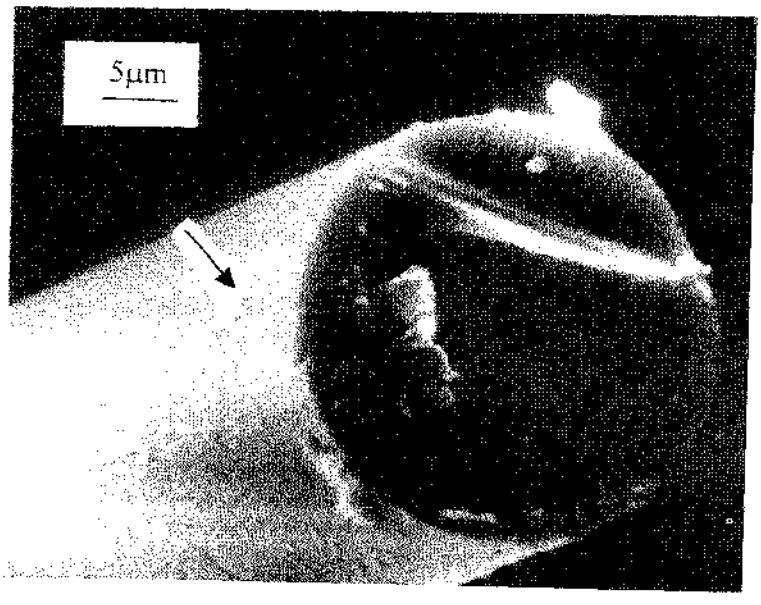

Figure 8 SEMicrograph depicting number of surface holes (indicated by an arrow) and the brittle nature of fibre exposed to 175° C for 1750 h.

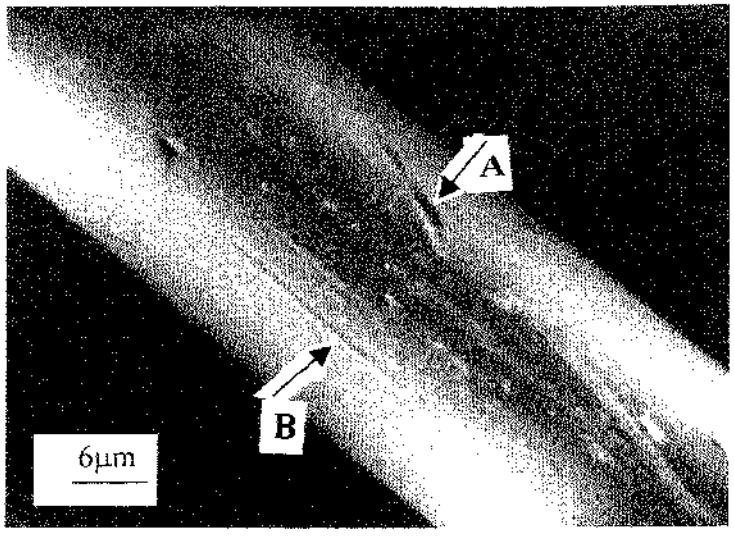

Figure 9 SEMicrograph showing groovelike features (A and B) on the surface of a fibre exposed to 175 C for 1750 h.

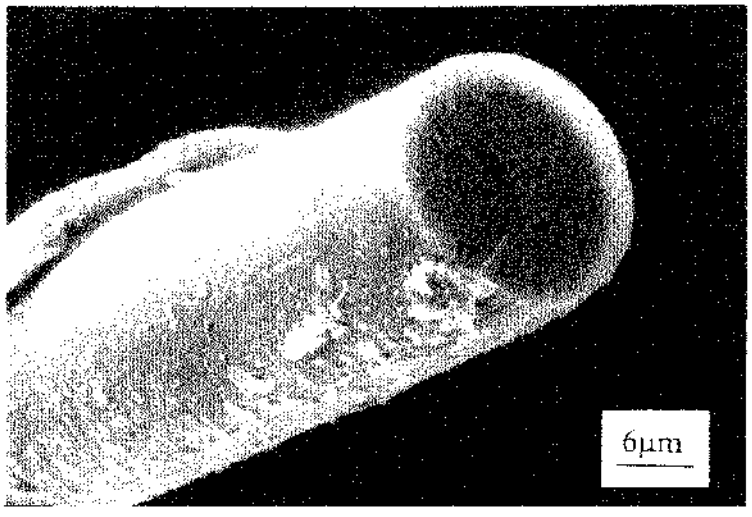

Figure 10 SEMicrograph showing material deposit engulfing the surface of a fibre exposed to 225°C for 22 h.

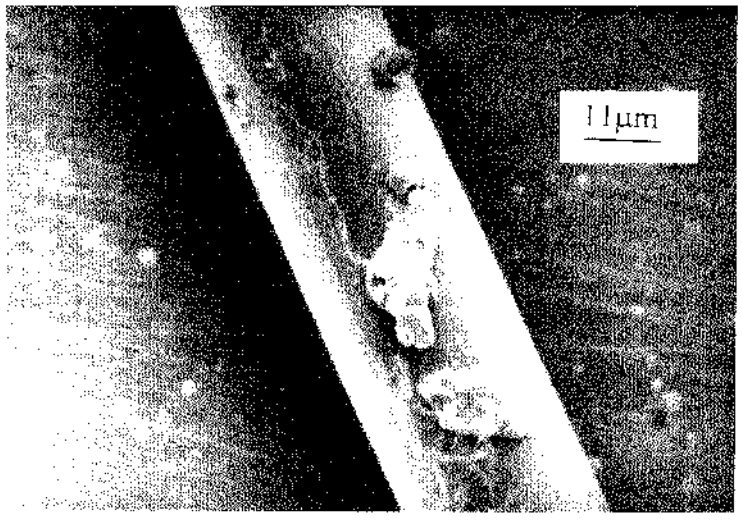

Figure 11 SEMicrograph showing increased material deposit on the surface of a Nylon 6.6 fibre exposed to 225°C for 22 h.

occurred. Details of the inner layers can also be seen in the micrograph. it may be mentioned that it is not unlikely that the line along which the damage has occurred corresponds to one of the lines observed on the surface of the as received fibre (Fig. 7a). In which case, the lines in Fig. 7a represent the initially, structurally weak or vulnerable regions which seem to have failed subsequently during heat treatment.

As in the case of fibres aged at 175°C, the fracture is of the brittle type for fibres aged at 225°C for 22 hours

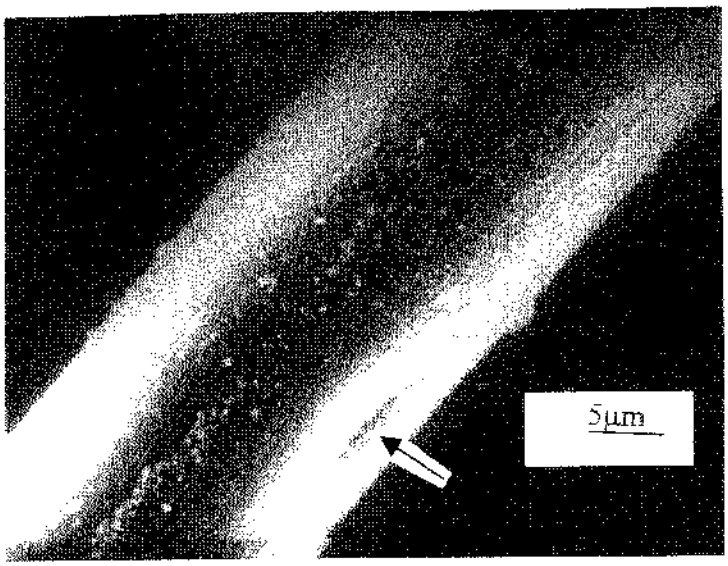

Figure 12 SEMicrograph depicting a localized deep pit indicated by an arrow on the surface of a fibre exposed to 225 °C for 22 h.

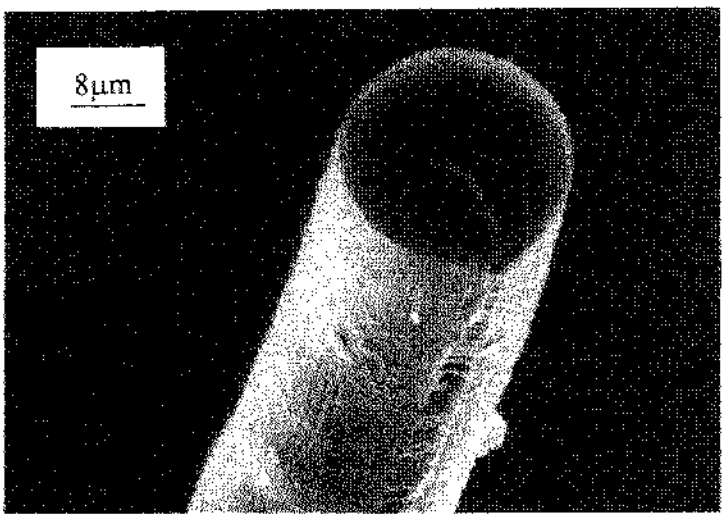

Figure 13 SEMicrograph showing a longitudinal degradation/failure on the surface of a fibre exposed to 225 °C for 22 h.

(Figs 10 and 13). Interestingly, the fractured end depicts a very smooth surface and a radial structure which bears a curious semblance to metallic materials.

3.3.4. Fibres aged at 245 °C

The staggeringly large quantities of surface deposits in fibres aged at 245 °C for 12 h can be seen in the micrograph presented in Fig. 14. The longitudinally disposed surface damage observed in fibres aged at 225 °C (Fig. 13) seems to have intensified at 245 °C (Fig. 15). The length over which this feature persists has also been registered in Figs 16 and 17. The split-open nature of the pit and the wavy nature of the crack can be clearly seen in the latter micrograph. As may be noticed from Figs 14 and 15 the fracture of fibres aged at 245 °C is also brittle in nature. The interesting features of the fractured end are the radial structure and the smooth section which were observed at 225 °C also.

Formation of [illegible] the surface of heat [illegible] fibres suggests [illegible] ageing some solid material has evolved from within the fibre via the holes and surface openings and have got deposited on the surface. The material could be associated with chemical degradation of the polymer induced during thermal ageing. As mentioned earlier, the present study does not include chemical analysis and therefore the products resulting from thermal degradation could not be identified. In addition to the solid deposits seen in the micrographs, gaseous components formed during heat treatment are also likely to have got evolved. The gaseous components can account for the weight loss described in Section 3.2, at least partially.

Thermally induced holes, pits and longitudinal discontinuities of the type described in this section can be expected to lead to deterioration in the initial tensile properties of the fibre. Details of the observed changes in the tensile properties are presented in the next section.

3.4. Tensile characteristics

As mentioned in the earlier sections, the observed changes in the crystal structural characteristics, weight loss and surface damages introduced by cumulative thermal ageing suggest deterioration from the initial tensile characteristics which indeed has been confirmed

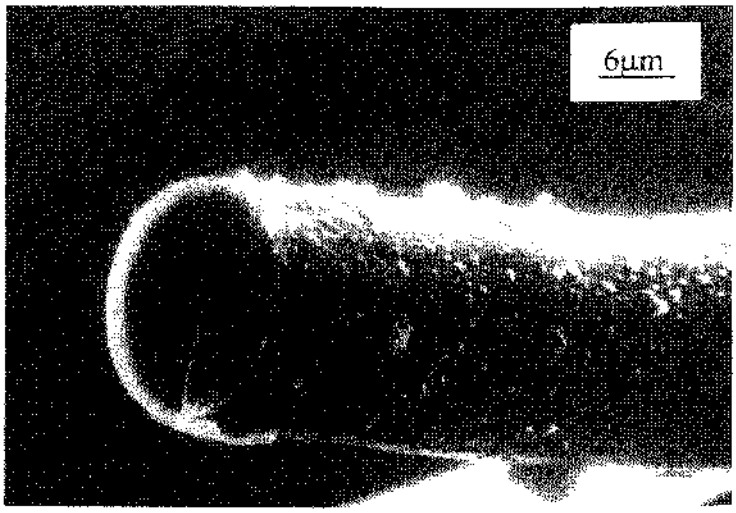

Figure 14 SEMicrograph showing large quantities of deposits on the surface of a fibre exposed to 245° C for 12 h.

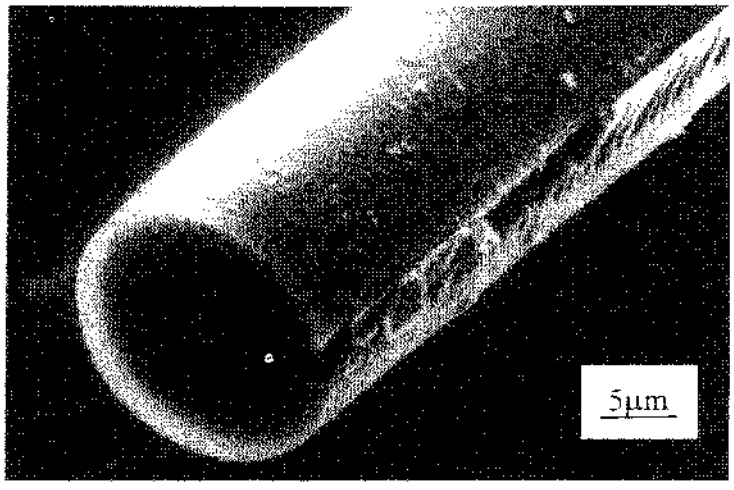

Figure 15 SEMicrograph showing longitudinally disposed damages on the surface of a fibre exposed to 245° C for 12 h.

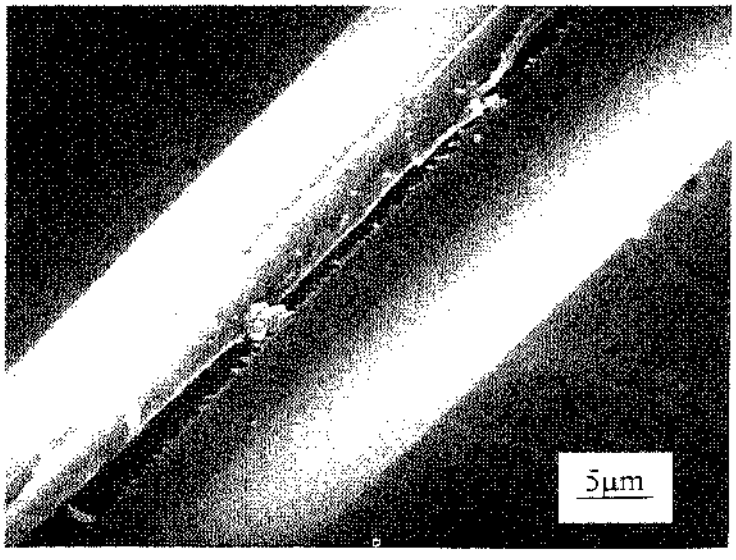

Figure 16 SEMicrograph showing the longitudinal damage in a fibre exposed to 245° C for 12 h.

experimentally. For the Nylon 6,6 fibres used in the present study, values of the initial tensile modulus (M_o), tensile strength (S_o) and elongation at break (ε_o) were 4.92(19), 0.78(2) GPa and 23(1)% respectively.

Fig. 18a and b present the typical load-extension curves. The former shows the effect of T and in the latter, the role of $t_{cum}(T)$ for a constant T has been depicted. The progressive changes in the slope and the

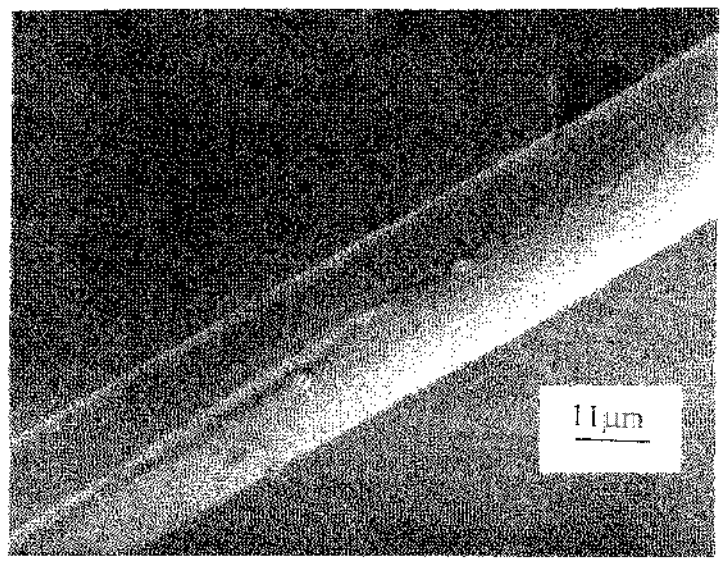

Figure 17 SEMicrograph showing the split-open nature of the surface damage (A) and wavy nature of a crack (B) on the surface of a fibre exposed to 245 °C for 12 h.

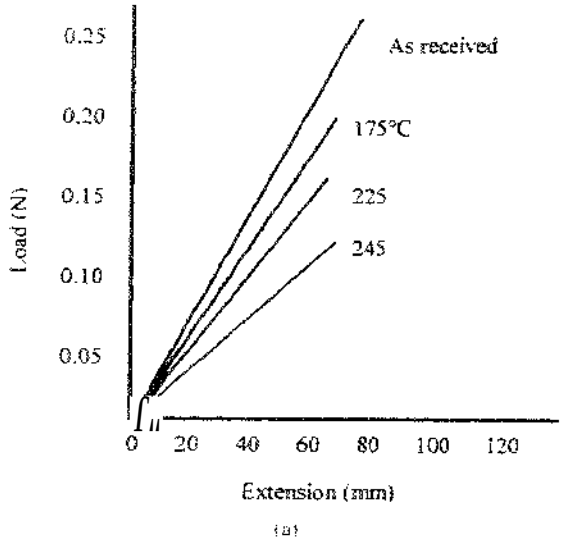

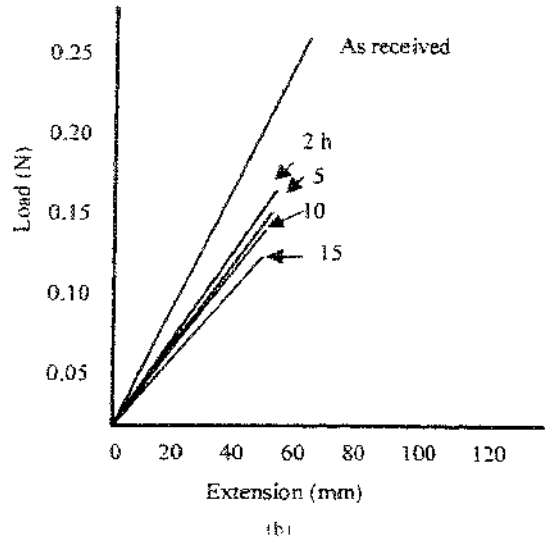

Figure 18 Typical load-extension curves recorded from individual Nylon 6,6 fibres prior to and after heat treatment. (a) As a function of T and (b) As a function of $t_{cum}(T)$ at 225 °C.

breaking load indicate that increase in temperature as well as $t_{cum}(T)$ lead to deterioration in the tensile modulus and strength respectively. Fig. 19a–c depict the respective thermally induced reductions in the tensile modulus, tensile strength and percentage elongation at break. Here, M_t^T, S_t^T, and ε_t^T represent the values of tensile modulus, strength and percentage elongation at break respectively for fibres exposed to temperature T for a duration of $t_{cum}(T)$. It may be noticed that after 800 h at 175 °C, the tensile modulus and strength decrease by ~40% and 70% respectively. At any stage of ageing at 175 °C, the reduction in the tensile strength is conspicuously more than the corresponding reduction in modulus. The preferential degradation of tensile strength suggests that the structural features connected with the tensile strength of the fibre deteriorate faster than those associated with the initial tensile modulus. It may be mentioned that Auerbach [16] has examined the kinetics of degradation of Nylon 6,6 yarn used in parachutes. His studies include the effects of temperature (in the range 90–150 °C) as well as the relative humidity in the range 0–100%.

In contrast with the behavior at 175 °C, fibres aged at 225 and 245 °C do not manifest such a preferential enhanced degradation in tensile strength. At these higher temperatures, both tensile modulus and strength appear to degrade by nearly equal amounts. The associated structural changes thus appear to occur simultaneously and perhaps in equal measures. As mentioned earlier in Section 3.1.2, reduction in tensile strength is accompanied by an increase in the angular separation between the equatorial reflections. A typical example has already been presented in Fig. 4. As in the case of tensile strength and modulus, the percentage elongation at break (Fig. 19c) also decreases with cumulative thermal exposure at any chosen temperature. At this stage, it must be pointed out that the structural and other changes found to occur in thermally aged Nylon 6,6 fibres are very similar to those found in thermally aged aramids, Kevlar, Twaron and Nomex [3–12]. The overall nature

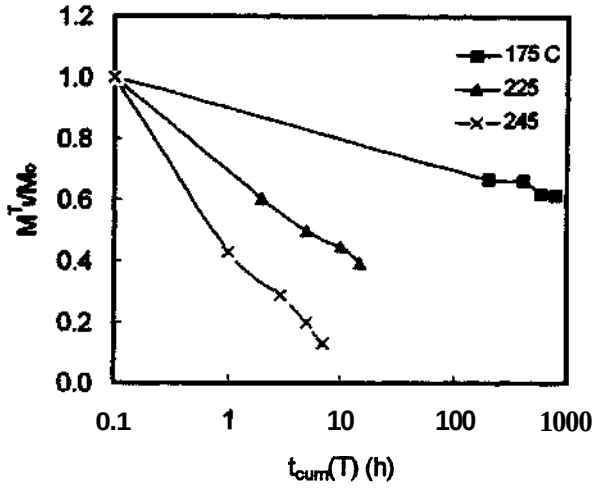

(a)

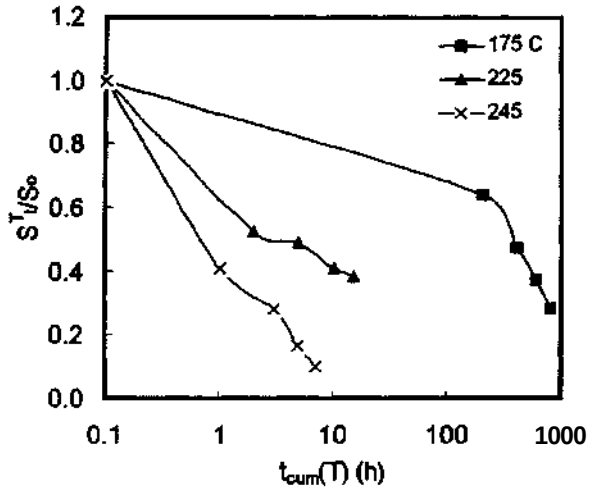

(b)

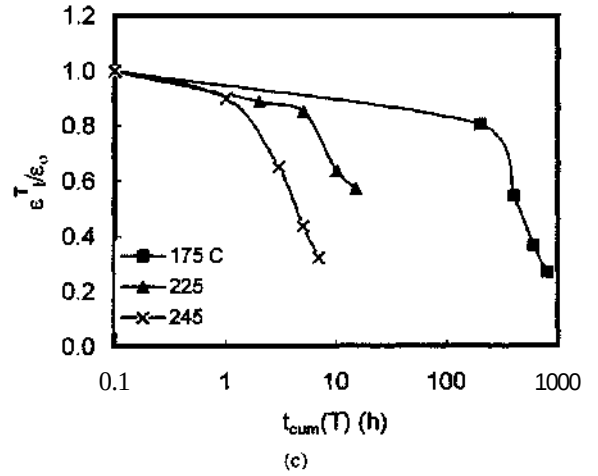

(c)

Figure 19 (a) Variation of M_t^T/M_o with $t_{cum}(T)$ and T. (b) Variation of S_t^T/S_o with $t_{cum}(T)$ and T. (c) Variation of $\varepsilon_t^T/\varepsilon_o$ with $t_{cum}(T)$ and T.

of the thermally induced effects thus appears to be common to aromatic as well as aliphatic polyamides.

4. Conclusions

The residual effects of thermal ageing on the initial characteristics of the aliphatic polyamide Nylon 6,6 include changes in the crystal structural as well as macro structural characteristics. The former includes conspicuous changes in X-ray crystallinity, unit cell dimensions and half widths. Thermal ageing introduces a progressive diminution and an eventual total loss in the crystallinity of the fibre. Macro changes include introduction of surface damages in the form of holes, material deposit and localized longitudinal deterioration. Thermal ageing also causes weight loss. The tensile modulus, strength and percentage elongation at break manifest reductions from the initial values. The results on Nylon 6,6 fibres indicate that the thermally induced changes are not exclusive to the aromatic polyamides. Similarities in the behavior of the aliphatic and the aromatic polyamides have been established.

Acknowledgement

The authors thank Dr. T. S. Prahlad, Director, NAL for the support. One of the authors (AJ) thanks the Naltech Pvt. Ltd, Bangalore, India for providing a contract post and the opportunity to work in the project. The authors wish to thank Dr. N. Balasubramanian and Mr. Basavaraj of Eternit Everest, India, for carrying out the tensile tests and Dr. T. A. Bhaskaran and Ms. Kalavati for recording the micrographs. The authors acknowledge the useful suggestions from Dr. R. V. Krishnan, Head, Materials Science Division, NAL.

References

1. W. J. ROFF and J. R. SCOTT, in "Fibres, Films, Plastics and Rubbers" (Butterworth, England, 1971) p. 216.
2. H. J. RADUSCH, M. STOLP and R. ANDROSCH, *Polymer* **35** (1994) 3568.
3. R. V. IYER and K. VIJAYAN, in "Polymer Science Recent Advances," Vol. 1, edited by I. S. Bhardwaj (Allied Publishers, New Delhi, India, 1994) p. 362.
4. *Idem.*, *Bull. Mater. Sci. 22* (1999) 1013.
5. R. V. IYER, Ph.D. Thesis, Bangalore University, Bangalore, India, 1999.
6. A. JAIN and K. VIJAYAN, *J. Mater. Sci.*, communicated.
1. *Idem.*, *ibid.* to be communicated.
8. A. JAIN, Ph.D. Thesis, Mangalore University, Mangalore, India, 2001.
9. R. V. IYER and K. VIJAYAN, in "Macromolecules New Frontiers," Vol. 2, edited by K. S. V. Srinivasan (Allied Publishers, New Delhi, India, 1998) p. 847.
10. *Idem.*, *Curr. Sci.* 75 (1998) 946.
11. *Idem.*, *J. Mater. Sci.* 35 (2000) 5731.
12. K. *VIJAYAN*, *Metals, Materials and Processes* **12** (2000) 259.
13. C. W. BUNN and E. V. GARNER, *Proc. Roy. Soc.* **189A** (1947) 39.
14. L. E. ALEXANDER, in "X-ray Diffraction Methods in Polymer Science" (Wiley-Interscience, New York, 1969) ch. 3.
15. M. SHUBHA, H. V. PARIMALA and K. VIJAYAN, *J. Mater. Sci. Lett.* **10** (1991) 1377.
16. H. AUERBACH, *J. Appl. Polym. Sci.* 37 (1989) 2213.

Received 25 October 2001
and accepted 30 January 2002